Electronic structure of Fe in some minerals, derived from iterative extended Hückel theory (IEHT), multiple scattering Xα (MS-Xα) calculations, and Mössbauer measurements

LAURENCE P. ALDRIDGE,* ECKHARD BILL, RAINER BLÄS, SIEGFRIED LAUER,
VISHNU R. MARATHE, ANDRZEJ SAWARYN, ALFRED X. TRAUTWEIN, HEINER WINKLER

Institut für Physik, Medizinische Universität, Ratzeburger Allee 160, D 2400 Lübeck 1,
Federal Republic of Germany

ABSTRACT

Optical transitions and the Mössbauer parameters isomer shift and quadrupole splitting have been compared with corresponding values computed from molecular orbital cluster calculations for ferric and ferrous ions in several minerals. Clusters comprised only Fe and the neighboring oxygen ions. Two molecular orbital methods—the iterative extended Hückel theory (IEHT) and the multiple scattering Xα (MS-Xα) method—were used.

Values derived from the IEHT method follow the trends that are predetermined by measured values, with the exception of the sign of the quadrupole interaction in gillespite. This failure is attributed to the inadequacy of the simple IEHT method to represent the electronic structure of gillespite. The situation considerably improves after taking into account configuration interaction among the five low-lying quintet states of the ferrous high-spin FeO_4^{6-} cluster.

The more sophisticated MS-Xα method has only been successful in describing optical data and isomer shifts, whereas calculated quadrupole splittings are unsatisfactory. Variations in the parameters did not improve this situation; therefore we suspect that the observed limitation of our MS-Xα results is due to the small cluster size used here.

INTRODUCTION

There have been many spectroscopic studies on the Fe sites in minerals using X-ray crystallography, polarized electronic spectroscopy, and Mössbauer spectroscopy. Each method enables the experimentalist to observe different aspects of the behavior of Fe. Since ligand field theory, which has often been used to interpret the electronic structure and hence the optical spectra (see Burns, 1970), suffers from some difficulties, Aldridge et al. (1982) calculated the electronic structure of ferrous ions in the minerals gillespite, garnet, and olivine by a semi-empirical molecular orbital method (iterative extended Hückel theory, IEHT). This method has the advantage that it is easy to handle and relatively economical of computer time. With the semi-empirical parameter set published earlier (Trautwein et al., 1975), the only parameters dependent on the mineral type were the positions of the ferrous ion and the neighboring oxygen atoms, which, however, were known from X-ray structure studies.

The IEHT method has also been successfully used to calculate the Mössbauer parameters quadrupole splitting (QS) and electron density at the Fe nucleus [$\rho(o)$] as a measure of the isomer shift (IS) of a large number of compounds (Marathe and Trautwein, 1983) including iron-

oxygen compounds (Trautwein et al., 1975; Reschke et al., 1977), ferrocene (Lauer et al., 1982), and iron halides (Grodzicki et al., 1981). In the present work, IEHT has been used to calculate the Mössbauer parameters QS and $\rho(o)$ for several minerals in the cluster approximation. The results from such a "cluster" calculation cannot be expected to give a completely accurate description of the minerals' electronic structure, and Winkler et al. (1983) have shown the effects that occur, e.g., in yttrium iron garnet (YIG), when the cluster size is increased. However, the calculations on large clusters (including up to 63 atoms) used many hours of computer time, and in addition the QS and $\rho(o)$ computed from the smallest clusters (i.e., FeO_6^{9-} and FeO_4^{5-}) were nearer to the values obtained from the largest clusters than to the values obtained from clusters of intermediate size. This is due to the fact that the point symmetry of Fe in intermediate-size clusters is not well preserved. Therefore, in this work, we restricted ourselves mainly to calculations on the smallest reasonable clusters, consisting of Fe and its nearest oxygen neighbors.

Tossell (1976), Tossell and Gibbs (1977), and Tossell et al. (1974) (and others cited in these papers) were the first to study Fe minerals by the multiple scattering Xα method, MS-Xα. They used clusters where Fe was in octahedral, tetrahedral, or square-planar coordination to oxygen, and they related the electronic structures of these models to those of minerals. More recently Tang Kai et al. (1980b) and Sherman (1984) have used the same meth-

---

* Present address: Chemistry Division, DSIR, Private Bag, Petone, New Zealand.
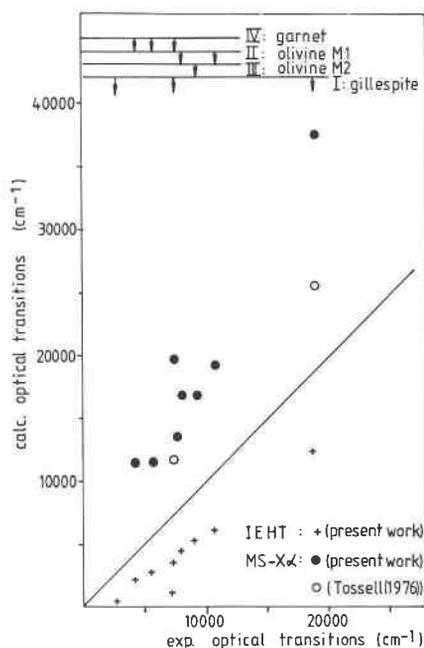
Fig. 1. Comparison of calculated and experimental optical transitions for some minerals. Experimental data are taken from (I) Burns et al. (1966); (II) and (III) Burns (1970, 1974) and Routcliffe (1976); (IV) Huggins (1975) and references therein.

Table 1. Parameters used in the MS-Xα calculations

no.	mineral	radius in a.u.	α	l_{max}	Watson sphere radius in a.u.
(I)	gillespite				
	outer sphere	5.8764	.73788	4	3.78
	Fe	2.4064	.71151	2	
	O	2.1264	.74447	1	
(II)	olivine M1				
	outer sphere	6.4983	.73976	4	4.212
	Fe	2.4985	.71151	2	
	O (a)	2.2267	.74447	1	
	O (b)	2.2181	.74447	1	
	O (c)	2.2858	.74447	1	
(III)	olivine M2				
	outer sphere	6.6574	.73976	4	4.330
	Fe	2.5022	.71151	2	
	O (a)	2.2997	.74447	1	
	O (b)	2.2179	.74447	1	
	O (c)	2.3246	.74447	1	
	O (d)	2.1904	.74447	1	
(IV)	garnet				
	outer sphere	6.8227	.74081	4	4.4665
	Fe	2.5680	.71151	2	
	O (a)	2.2589	.74447	1	
	O (b)	2.3562	.74447	1	

od to calculate the bonding of Mn in minerals. We were interested to learn if the MS-Xα method would correctly describe (1) the energies of optical transitions and (2) the parameters QS and $\rho(o)$ for a series of minerals with different geometries when we again use the smallest cluster with Fe and its oxygen neighbors only.

CALCULATION METHODS

The full details of the IEHT method have already been published (Trautwein et al., 1975; Grodzicki et al., 1981). Our present application differs from that of Aldridge et al. (1982) in that (1) we used here the IEHT parameters tabulated in the paper by Grodzicki et al. (1981) with the single exception of ϵ_O for oxygen [following Trautwein et al. (1975), we used 50 eV for oxygen $2s$ and 33 eV for oxygen $2p$] and (2) we used open-shell electronic configurations ($S = 2$ for ferrous or $S = 2.5$ for ferric systems). These provisions improved both the ease and speed of convergence. It took less than 5 min of CPU time on a VAX11/750 for each IEHT calculation to converge to a self-consistent charge of maximum deviation of less than 0.01 of an electron. The Mössbauer parameters were calculated from the IEHT wavefunctions in the manner described by Grodzicki et al. (1981) with the improvements by Lauer et al. (1982).

For the MS-Xα calculations, we have used the program by Cook and Case (1983), where the Mössbauer parameters were calculated from the one-electron package using the charge-partitioning scheme of Case and Karplus (1976). By "optimizing" the MS-Xα parameters for each com-

pound, it would have been possible to obtain calculated optical energies that would give better absolute agreement with experiment. Tossell (1976) has in fact achieved a better agreement for the optical spectrum of gillespite than we did (Fig. 1) by using in his MS-Xα calculations a FeO_4^{6-} cluster with D_{4h} symmetry and touching spheres. It was shown by Aizman and Case (1981) and by De Siqueira et al. (1975) how orbital energies and also Mössbauer parameters depend on MS-Xα parameters. However, since we were interested in obtaining results that could be directly compared over a series of minerals, we wanted to be independent from variations of MS-Xα parameters as much as possible. Therefore we have used the automatic features of the program by Cook and Case (1983) to determine overlapping sphere sizes. The Watson sphere size was chosen in the same way as by Tossell et al. (1977) and Tossell (1974), i.e., so that the Watson sphere passes through the center of the oxygen atom farthest away from the Fe. Table 1 includes the parameters that have been used in our MS-Xα calculations. To reach convergence of 0.0001 a.u. in the potential, the SCF part of the MS-Xα program took about 40 min for a FeO_4^{6-} cluster (gillespite), and between 4 and 6 h for the FeO_6^{10-} cluster (olivine) and FeO_8^{14-} cluster (garnet). Virial ratios ranged from -2.001 to -2.005 for these clusters.

RESULTS AND DISCUSSION

The origin of the crystal structure data of the minerals under study here is given in Table 3. We have selected these crystal structures to generate the coordinates of our

Table 2. Characterization of the spin-up and spin-down valence orbitals as derived from MS-Xα calculations

sym. repres.	energy	occup.	Fe s	Fe p	Fe d	Oa s	Oa p	Ob s	Ob p	sym. repres.	energy	occup.	Fe s	Fe p	Fe d	Oa s	Oa p	Ob s	Ob p
A	-2.810	1.0	3	0	0	58	0	37	0	A	-2.802	1.0	2	0	0	53	0	43	0
B2	-2.777	1.0	0	2	0	97	0	0	0	B2	-2.766	1.0	0	1	0	97	0	0	0
B3	-2.765	1.0	0	1	0	4	0	93	0	B3	-2.762	1.0	0	1	0	3	0	95	0
B1	-2.764	1.0	0	1	0	45	0	52	0	B1	-2.758	1.0	0	1	0	38	0	59	0
B2	-2.737	1.0	0	0	0	0	0	98	0	B2	-2.733	1.0	0	0	0	0	0	98	0
A	-2.736	1.0	0	0	1	38	0	59	0	A	-2.729	1.0	0	0	1	43	0	54	0
B3	-2.732	1.0	0	0	1	93	0	4	0	B3	-2.720	1.0	0	0	1	95	0	3	0
B1	-2.706	1.0	0	0	0	53	0	46	0	B1	-2.698	1.0	0	0	0	59	0	39	0
A	-1.911	1.0	0	0	19	0	46	0	34	A	-1.894	1.0	0	0	5	0	51	0	43
B1	-1.910	1.0	0	0	18	0	44	0	36	B1	-1.893	1.0	0	0	4	0	50	0	44
A	-1.859	1.0	11	0	10	1	57	0	18	A	-1.839	1.0	12	0	0	0	35	2	48
A	-1.855	1.0	6	0	14	0	22	2	54	B3	-1.839	1.0	0	5	0	0	50	3	40
B3	-1.850	1.0	0	2	19	0	49	1	26	A	-1.835	1.0	3	0	2	1	54	0	38
B2	-1.845	1.0	0	0	26	0	42	1	30	B1	-1.828	1.0	0	6	0	1	40	1	50
B1	-1.832	1.0	0	6	0	1	43	1	46	B2	-1.826	1.0	0	0	1	0	72	0	25
B3	-1.829	1.0	0	3	22	0	27	1	45	B2	-1.814	1.0	0	5	0	2	51	0	40
B2	-1.821	1.0	0	5	2	2	73	0	17	B3	-1.809	1.0	0	0	1	0	15	0	82
B2	-1.797	1.0	0	1	23	0	23	0	51	B3	-1.769	1.0	0	0	3	0	36	0	59
B3	-1.796	1.0	0	0	10	0	28	0	60	B2	-1.762	1.0	0	0	3	0	51	1	43
A	-1.786	1.0	0	0	33	0	27	0	39	A	-1.741	1.0	0	0	3	0	43	0	52
B3	-1.741	1.0	0	0	16	0	19	0	62	B2	-1.702	1.0	0	4	2	0	66	0	26
B2	-1.737	1.0	0	1	14	0	61	0	21	B1	-1.694	1.0	0	3	0	0	34	0	61
B1	-1.733	1.0	0	0	69	0	14	0	15	B3	-1.691	1.0	0	2	0	0	26	0	70
A	-1.724	1.0	0	0	51	0	6	0	42	B3	-1.676	1.0	0	0	12	0	64	0	23
A	-1.715	1.0	0	0	43	0	43	0	13	B2	-1.674	1.0	0	0	1	0	13	0	85
B1	-1.698	1.0	0	3	3	0	29	0	63	A	-1.668	1.0	0	0	8	0	43	0	47
B2	-1.696	1.0	0	3	5	0	56	0	33	B1	-1.667	1.0	0	0	0	0	36	0	63
B3	-1.695	1.0	0	2	0	0	27	0	69	B2	-1.661	1.0	0	0	5	0	33	0	60
B2	-1.675	1.0	0	0	0	0	30	0	69	A	-1.656	1.0	0	0	1	0	52	0	46
B1	-1.671	1.0	0	0	0	0	38	0	60	B3	-1.639	1.0	0	0	0	0	81	0	16
A	-1.662	1.0	0	0	0	0	51	0	47	B1	-1.636	1.0	0	0	0	0	69	0	29
B3	-1.647	1.0	0	0	0	0	74	0	24	B1	-1.619	1.0	0	0	4	0	51	0	43
B1	-1.642	1.0	0	0	0	0	71	0	28	A	-1.408	1.0	0	0	49	19	3	23	4
B1	-1.602	1.0	0	0	10	0	46	0	42	A	-1.387	0	0	0	63	13	0	19	2
B2	-1.591	1.0	0	0	31	0	1	0	66	B1	-1.376	0	0	0	91	0	4	0	2
A	-1.580	1.0	0	0	32	0	30	0	36	B2	-1.333	0	0	0	88	0	0	1	10
B3	-1.567	1.0	0	0	35	1	61	0	1	A	-1.325	0	0	0	86	1	4	0	6
A	-1.387	0	0	0	0	40	1	53	3	B3	-1.310	0	0	0	85	2	11	0	0
B2	-1.232	0	0	1	0	62	5	8	22	B2	-1.239	0	0	1	0	62	5	8	22
B3	-1.220	0	0	1	0	5	19	66	8	B3	-1.226	0	0	0	0	5	19	66	8
A	-1.216	0	0	0	8	26	12	28	23	A	-1.222	0	0	0	3	30	10	32	22
B1	-1.173	0	0	0	4	17	19	31	27	B1	-1.180	0	0	0	1	18	17	34	27

Note: All energies are in rydbergs. The occupancy gives the number of electrons in a molecular orbital (MO). The symmetry representation corresponds to the transformed coordinates (in atomic units) where Fe is at 0, 0, 0; Oa is at 0.7351, 3.4571, 2.2527; and Ob is at 3.6077, −0.6054, 2.5627.

iron-oxygen clusters that contained the greatest amount of Fe in the appropriate site. The influence of structural changes is illustrated, for example, by the calculated QS of Fe^{3+} in the M3 epidote site. The IEHT value derived from allanite containing 12% Fe^{3+} and 72% Fe^{2+} (Dollase, 1971, 1973) was 1.16 mm·s⁻¹, compared to 0.86 mm·s⁻¹ derived from epidote containing 85% Fe^{3+} (Gabe et al., 1973).

From the IEHT calculations of the four reference clusters (gillespite, olivine M1 and M2, and garnet) originally studied by Aldridge et al. (1982), we found that the molecular orbitals (MOs) indeed reflect a ferrous high-spin state, with identical ordering of orbitals as observed by Aldridge et al. (1982). We then used the approximation to calculate the optical transitions from the energy difference between MOs having predominant d character. The comparison between the calculated and experimental transitions is made in Figure 1, and an approximately linear relationship is observed except for the case of the gillespite 7500 cm⁻¹ band. The optical transitions were also calculated with the spin-polarized MS-Xα routine using Slater's transition-state method. We again observe an almost linear relationship between calculated and experimental transitions (Fig. 1). In gillespite, the ordering of the lowest unoccupied molecular orbitals (LUMOs) is identical to the situation in the IEHT results. But for olivine and garnet, we found from the MS-Xα calculations an extra MO within the sequence of the LUMOs with the same d-character
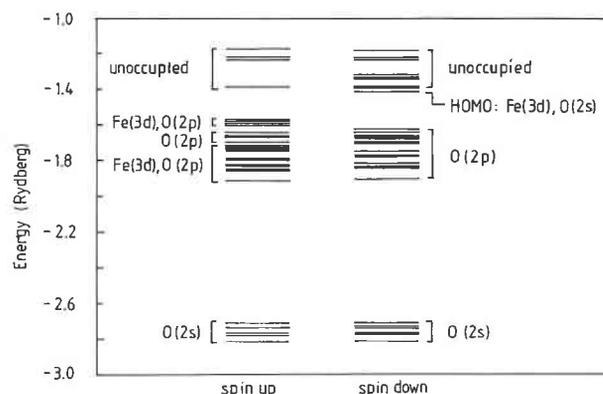
Fig. 2. MS-Xα valence electronic structure of FeO_8^{4-} (IV: garnet).

Table 3. Details of experimental and calculated (IEHT) Mössbauer parameters and structures of mineral clusters

no.	mineral	site	coord. of Fe	exp.sign of efg	QS^{exp} (mms^{-1})			$IS^{exp}_{\alpha-Fe}$ (mms^{-1})			Ref.of exp.data	$QS^{calc,IEHT}$ (mms^{-1})	cluster for MO-calc.	Ref.for structure
					4.2K	80K	300K	4.2K	80K	300K				
I	gillespite	Fe^{2+}	4	+		0.56	0.51		0.84	0.76	a	−0.84	FeO_4^{6-}	j
												−0.04(IEHT-CI)	FeO_4^{6-}	j
II	olivine	M1,Fe^{2+}	6				2.89			1.16	b		FeO_6^{10-}	
				+	3.07	2.86	2.60	1.30	1.23	1.16	c	+3.19	FeO_6^{10-}	k
III	olivine	M2,Fe^{2+}	6				2.90			1.17	b			
				+	3.08	3.10	2.89	1.22	1.22	1.16	c	+3.20	FeO_6^{10-}	k
IV	garnet	Fe^{2+}	8				3.53			1.30	b			
				−			3.53			1.29	c,d	−3.23	FeO_8^{14-}	l
V	garnet	Fe^{3+}	6	+	0.55			0.39			d,e	+0.13	FeO_6^{9-}	m
VI	YIG	Fe^{3+}	4	−		0.89			0.15		f	−0.69	FeO_4^{5-}	f
												−0.56	63 atoms	f
VII	YIG	Fe^{3+}	6	−		0.41			0.38		f	−0.76	FeO_6^{9-}	f
												−0.21	57 atoms	f
VIII	ferrosilite	M1,Fe^{2+}	6			3.13	2.49		1.31	1.18	g	+3.29	FeO_6^{10-}	n
IX	ferrosilite	M2,Fe^{2+}	6			2.00	1.91		1.27	1.13	g	+2.75	FeO_6^{10-}	n
X	epidote	M3,Fe^{3+}	6				2.05			0.36	h	−0.86	FeO_6^{9-}	o
												−1.16	FeO_6^{9-}	p
XI	epidote	M3,Fe^{2+}	6				1.67			0.90	h	+2.55	FeO_6^{10-}	p
XII	biotite	M1,Fe^{2+}	6				2.58			1.07	i	+3.03	FeO_6^{10-}	q
XIII	biotite	M2,Fe^{2+}	6				2.14			1.06	i	+3.00	FeO_6^{10-}	q

(a) Clark et al. (1967). (b) Bancroft et al. (1967). (c) Routcliffe (1976); fayalite (synthetic). (d) Amthauer et al. (1976). (e) Murad (1984); T = 121 K. (f) Winkler et al. (1983). (g) Dowty and Lindsley (1973). (h) Dollase (1973); samples HU and PC. (i) Hogg and Mead (1970); sample 6. (j) Hazen and Finger (1983); gillespite at 1 bar. (k) Birle et al. (1968); fayalite. (l) Prandl (1971). (m) Novak and Gibbs (1971); andradite. (n) Burnham (1966). (o) Gabe et al. (1973). (p) Dollase (1971); allanite. (q) Bohlen et al. (1980); biotite.

Abbreviations used: electric field gradient (efg), quadrupole splitting (QS), isomer shift (IS).
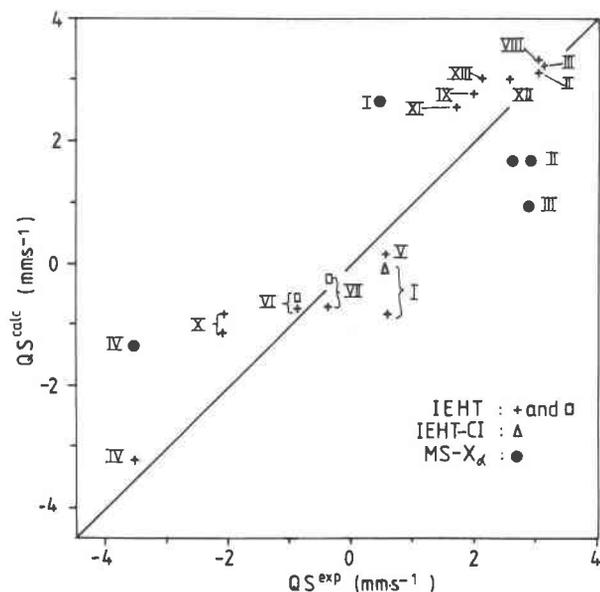
Fig. 3. Comparison of calculated (IEHT and MS-Xα) and experimental quadrupole splittings QS. The sign of QS corresponds to the electric field gradient. Calculated IEHT values indicated by + correspond to large cluster sizes. The IEHT-CI value obtained for FeO_4^{6-} (gillespite) is indicated by Δ. As experimental values, low-temperature data (if available) have been used, because at 300 K, spin-orbit coupling might reduce QS considerably compared to at 4.2 K (see Table 3).

as the highest occupied molecular orbital (HOMO). However, no optical transition takes place to this MO.

As an example for the calculated electronic structure of valence orbitals, we discuss the FeO_8^{14-} cluster (IV: garnet) in more detail. The characterization of MS-Xα molecular orbitals in terms of atomic orbitals (AOs) was obtained using the charge-partitioning method (Case and Karplus, 1976) to generate single-center orbitals. The energies of
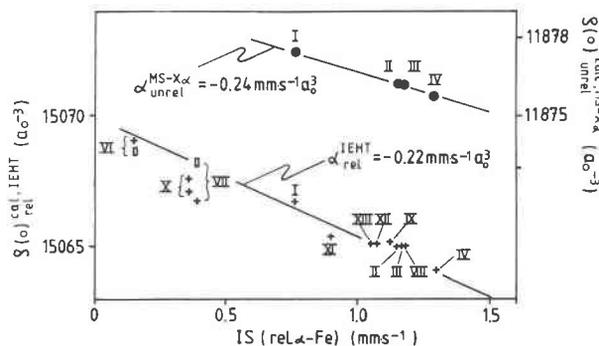
Fig. 4. Comparison of calculated (IEHT and MS-Xα) electron densities at the Fe nucleus ρ(o) with experimental isomer shifts δ. All experimental data refer to 300 K (see Table 1). Calculated IEHT values indicated by □ correspond to large cluster sizes. Correcting the unrelativistic Ms-Xα values with the scaling factor S = 1.3 yields $\alpha^{MS-X} = -0.185$ mm·s$^{-1}a_0^3$.
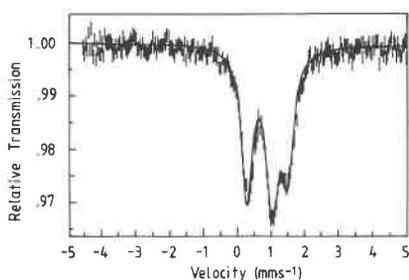
Fig. 5. Experimental Mössbauer spectrum of gillespite obtained at 100 K under externally applied magnetic field of 6.74 T, which was applied parallel to the γ-beam. The spin-Hamiltonian analysis (solid line) yields QS = +0.56 mm·s⁻¹ assuming complete alignment of the crystalline c axis perpendicular to the magnetic field.

Table 4. IEHT orbital occupancies of Fe AOs derived for FeO_4^{6-}; I: gillespite

	IEHT	IEHT-CI
x^2-y^2	1.17	1.20
z^2	1.95	1.90
xz,yz	1.04	1.01
xy	1.08	1.04
p_z	0.38	0.25
$p_{x,y}$	0.14	0.15

the occupied valence orbitals comprise several bands, which are shown in Figure 2 and which are identified in Table 2 by their symmetry representations and AO character. IEHT results differ from MS-Xα results significantly: (1) Fe(3d)–O(2p) interaction is restricted mainly to the 4 highest singly occupied IEHT MOs, whereas the MS-Xα procedure yields more than 15 MOs with Fe(3d)–O(2p) character; (2) Fe(3d)–O(2s) interaction is reflected by the 4 highest doubly occupied IEHT MOs, whereas the HOMO of spin-up orbitals only represents Fe(3d)–O(2s) character within the MS-Xα electronic structure. These differences in electron distribution among AOs as derived from the IEHT and MS-Xα method, respectively, are also reflected by the calculated quadrupole splittings (see below).

We have derived QS and ρ(o) for clusters I to XIII using the IEHT method and for clusters I to IV using the MS-Xα method. When comparing calculated and experimental data (Figs. 3 and 4 and Table 3), we observe that IEHT values follow the trend that is predetermined by measurement, with the exception of QS of gillespite. To make sure that the disagreement of QS$^{calc, IEHT}$ and QS^{exp} in gillespite is not due to ambiguities of the sign determination of quadrupole interaction, we performed a series of Mössbauer experiments (with various applied magnetic fields at different temperatures) on a polycrystalline gillespite sample, which exhibited a considerable degree of alignment although it was ground together with sugar in order to avoid preferred orientation. The spin-Hamiltonian analysis of the obtained spectra (one example is shown in Fig. 5), however, unambiguously revealed that the electric field gradient (efg) is positive, in agreement with the result of Clark et al. (1967). Having established the sign of the efg, we looked for reasons for the disagreement between QS^{calc} and QS^{exp}, and we tried to refine the calculations:

1. The four negatively charged oxygen ions ($q_{ox} = -1.64e$) in the x-y-plane of the cluster are not sufficient to balance the dominating negative contribution to the efg that arises from the (doubly occupied) nonbonding Fe $3d_z$ orbital within the ferrous high-spin state of FeO_4^{6-}. An ab initio calculation on FeO_4^{6-} with GAUSSIAN 82 using the Huzinaga basis set yields practically the same result. However,

when Fe 4p,4d AOs are added to this basis set, the efg becomes positive with QS taking the value of about 1.5 mm·s⁻¹.

2. Extending the cluster size from FeO_4^{6-} by including neighboring ions up to a distance of 5 Å from the central Fe changes QS$^{calc, IEHT}$ from −0.84 to −1.23 mm·s⁻¹ and hence does not improve the situation, contrary to the case with YIG (VI and VII in Table 1) treated by Winkler et al. (1983).

3. By applying configuration interaction (CI) among the five IEHT-MO quintet states $^5A_{1g}$, ^5E_g, $^5B_{2g}$, and $^5B_{1g}$, we arrive for the FeO_4^{6-} cluster at QS$^{calc, IEHT-CI}$ = −0.04 mm·s⁻¹, which is closer to QS^{exp} than QS$^{calc, IEHT}$. Compared to the value of QS$^{calc, IEHT}$, in QS$^{calc, IEHT-CI}$ (a) the negative Fe 3d,4p contribution is smaller by about 0.6 mm·s⁻¹ owing to changes in the Fe 3d,4p orbital occupancies as seen in Table 4 and (b) the positive overlap and ligand contributions are larger by about 0.2 mm·s⁻¹ owing to slightly more negative charges q_{ox} at the four oxygen ligands ($q_{ox} = -1.70e$).

We recall that our former IEHT-CI calculation on FeO_4^{6-} (Trautwein et al., 1975) yielded QS^{calc} = +0.35 mm·s⁻¹ only because we used a nuclear quadrupole moment too large ($Q = 0.21$ barn); here we took the more appropriate value $Q = 0.16$ barn.

The Δδ-Δρ(o)^{IEHT} relation in Figure 4 yields the value −0.22 mm·s⁻¹a_0^3 for the isomer-shift calibration constant $α = Δδ/Δρ(o)^{IEHT}$, close to the value that we have obtained from IEHT studies of iron-halide ($α = -0.21$ mm·s⁻¹a_0^3; Sanchez et al., 1979), iron-oxygen ($α = -0.2$ mm·s⁻¹a_0^3; Reschke et al., 1977), iron-sulfur ($α = -0.25$ mm·s⁻¹a_0^3; Trautwein et al., 1985), and other iron-containing compounds ($α = -0.21$ mm·s⁻¹a_0^3; Marathe and Trautwein, 1983).

Our MS-Xα results of QS for clusters I to IV do not match with experimental data, whereas the Δδ-Δρ(o)$^{MS-Xα}$ relation (after correcting for relativistic contributions) yields the value −0.185 mm·s⁻¹a_0^3 for the isomer-shift calibration constant $α^{MS-Xα}$, which is in reasonable agreement with other trends (see the $α^{IEHT}$ values from above and the $α_{rel}^{MS-Xα}$ value of −0.215 mm·s⁻¹a_0^3 reported by

Tang Kai et al. (1980a) for FeO_4^{5-} clusters). From this, we conclude that the gross population of Fe $3d$ and Fe $4s$ shells as derived from the MS-Xα method is realistic; however, the distribution of charges among the five Fe $3d$ orbitals is not well represented. We carried out a number of test calculations to check how dependent the QS of gillespite is on the choice of parameters of the MS-Xα method. Variations of the sphere radii by 8%, of the Watson sphere by 50% and of the l-quantum number (which is equivalent to the inclusion of Fe f and oxygen d orbitals) caused changes in efg by 10%, 13%, and 2%, respectively. Thus it seems that the limitations of our MS-Xα calculations are more likely due to the cluster approach than to the calculation procedure itself.

CONCLUSIONS

1. Simple IEHT calculations of clusters containing only Fe ions surrounded by their oxygen neighbors can be used to correlate the calculated and experimental optical and Mössbauer parameters of Fe in most tetrahedral, octahedral, or 8-coordinated Fe sites within minerals.

2. The IEHT method may fail sometimes, as the case of gillespite—which has square-planar coordination—has shown.

3. Using the more sophisticated MS-Xα method has not been altogether successful. Despite the reasonable agreement between the optical spectra and the calculated transitions, and the linear relationship between charge densities at the Fe nucleus and the isomer shifts, the results for the quadrupole splitting were not satisfactory, and we believe that this is due to the inadequacy of the cluster approach. We expect that better agreement between calculated and experimental QS can only be achieved when the effect of the bonding of the oxygen atoms to the silicate lattice is considered. In the IEHT calculations, this is not as a severe problem as in the MS-Xα calculations, because within the IEHT method, the ionization potentials of oxygen are parametrized such that they implicitly take care of charges that lie outside the clusters actually used.

REFERENCES

Aizman, A., and Case, D.A. (1981) Xα multiple scattering study of hexacyanoferrate (III). Inorganic Chemistry, 20, 528–533.

Aldridge, L.P., Tse, J.S., and Bancroft, G.M. (1982) The identification of Fe^{2+} in the M4 site of the calcic amphiboles: Discussion. American Mineralogist, 67, 335–339.

Amthauer, G., Annersten, H., and Hafner, S.S. (1976) The Mössbauer spectrum of ^{57}Fe in silicate garnets. Zeitschrift für Kristallographie, 143, 14–55.

Bancroft, G.M., Maddock, A.G., and Burns, R.G. (1967) Applications of the Mössbauer effect to silicate mineralogy—Iron silicates of known crystal structure. Geochimica et Cosmochemica Acta, 31, 2219–2246.

Birle, J.D., Gibbs, G.V., Moore, P.B., and Smith, J.V. (1968) Crystal structures of natural olivines. American Mineralogist, 53, 807–824.

Bohlen, S.R., Peacor, D.R., and Essene, E. J. (1980) Crystal chemistry of a metamorphic biotite and its significance in water barometry. American Mineralogist, 65, 55–62.

Burnham, C. V. (1966) Ferrosilite. Carnegie Institution of Washington Year Book 65, 285–290.

Burns, R.G. (1970) Mineralogical applications of crystal field theory. Cambridge University Press.

——— (1974) The polarized spectra of iron in silicates: Olivine. A discussion of neglected contributions from the Fe^{2+} ion in M(1) sites. American Mineralogist, 59, 625–629.

Burns, R.G., Clark, M.G., and Stone, A.J. (1966) Vibronic polarization in the electronic spectra of gillespite. A mineral containing iron (II) in square-planar coordination. Inorganic Chemistry, 5, 1268–1272.

Case, D.A., and Karplus, M. (1976) The calculation of one-electron properties from Xα multiple scattering wavefunctions. Chemical Physics Letters, 39, 33–38.

Clark, M.G., Bancroft, G.M., and Stone, A.J. (1967) Mössbauer spectrum of Fe^{2+} in a square-planar environment. Journal of Chemical Physics, 47, 4250–4261.

Cook, M., and Case, D.A. (1983) XASW: Atomic Xα and molecular scattering Xα electronic structure calculations. Quantum Chemistry Program Exchange, Program No. 465.

De Siqueira, M.L., Larsson, S., and Conolly, J.W.D. (1975) Mössbauer isomer shifts and the multiple-scattering method. Journal of Physics and Chemistry of Solids, 36, 1419–1422.

Dollase, W.A. (1971) Refinement of the crystal structures of epidote, allanite and hancockite. American Mineralogist, 56, 447–476.

——— (1973) Mössbauer spectra and iron distribution in the epidote-group minerals. Zeitschrift für Kristallographie, 138, 41–63.

Dowty, E., and Lindsley, D.H. (1973) Mössbauer spectra of synthetic hedenbergite-ferrosilite pyroxenes. American Mineralogist, 58, 850–868.

Gabe, E.J., Portheine, J.C., and Whitlow, S.H. (1973) A reinvestigation of the epidote structure: Confirmation of the iron location. American Mineralogist, 58, 218–223.

Grodzicki, M., Lauer, S., Trautwein, A.X., and Vera, A. (1981) Applications of molecular orbital calculations to Mössbauer and NMR spectroscopy of halogen-containing compounds. In J.D. Stevens and G.K. Shenoy, Eds. Recent chemical applications of Mössbauer spectroscopy. American Chemical Society Advances in Chemistry Series 194.

Hazen, R.H., and Finger, L.W. (1983) High-pressure and high-temperature study of gillespite I-II phase transition. American Mineralogist, 68, 595–603.

Hogg, C.S., and Mead, R.E. (1970) The Mössbauer spectra of several micas and related minerals. Mineralogical Magazine, 37, 606–614.

Huggins, F.E. (1975) The $3d$ levels of ferrous ions in silicate garnets. American Mineralogist, 60, 316–319.

Lauer, S., Grodzicki, M., Trautwein, A.X., Vera, A., Osborne, A.G., Whiteley, R.H., and Stoeckli-Evans, R. (1982) Mössbauer and molecular orbital investigation of ferrocene and 1-ferrocenphanes. In V.R. Bhide, Ed. Indian National Science Academy, Proceedings, Physical Sciences, Special Volume, International conference on the application of the Mössbauer effect, 1981, Jaipur, India, 774–776. Indian National Science Academy, New Delhi.

Marathe, V.R., and Trautwein, A.X. (1983) Calculation of charge density, electric field gradient and internal magnetic field at the nuclear site using molecular orbital cluster theory. In B.V. Thosar and P.K. Iyengar, Eds. Mössbauer spectroscopy: applications to physics, chemistry, and biology. Elsevier.

Murad, E. (1984) Magnetic ordering in andradite. American Mineralogist, 69, 722–724.

Novak, G.A., and Gibbs, G.V. (1971) The crystal chemistry of silicate garnets. American Mineralogist, 65, 791–825.

Prandl, W. (1971) Die magnetische Struktur und die Atomparameter des Almandins $Al_2Fe_3(SiO_4)_3$. Zeitschrift für Kristallographie, 134, 333–343.

Reschke, R., Trautwein, A.X., and Desclaux, J.P. (1977) Limitation of semi-empirical MO-calculations in deriving charge densities $\rho(o)$ in iron-oxygen compounds. Journal of Physics and Chemistry of Solids, 38, 837–841.

Routcliffe, P. (1976) A Mössbauer study of ferrous silicates. Ph.D. thesis, Australian National University.

Sanchez, J.P., Friedt, J.M., Trautwein, A.X., and Reschke, R. (1979) Electronic charge and spin distribution in some iron halides from the interpretation of the ^{57}Fe and ^{129}I hyperfine interactions. Physical Review B, 19, 365–378.

Sherman, D.M. (1984) The electronic structures of manganese oxide minerals. American Mineralogist, 69, 788–799.

Tang Kai, A., Annersten, H., and Ericsson, T. (1980a) Molecular orbital (MSXα) calculations of s-electron densities of tetrahedrally coordinated ferric iron: Comparison with experimental isomer shifts. Physics and Chemistry of Minerals, 5, 343–349.

Tang Kai, A., Larsson, S., and Halenius, U. (1980b) The electronic structure and absorption spectrum of MnO_6^{8-} octahedra in manganian andalusite. Physics and Chemistry of Minerals, 6, 77–84.

Tossell, J.A. (1976) Electronic structures of iron-bearing oxide minerals at high pressure. American Mineralogist, 61, 130–144.

Tossel, J.A., and Gibbs, G.V. (1977) Molecular orbital studies of geometries and spectra of minerals and inorganic compounds. Physics and Chemistry of Minerals, 2, 21–57.

Tossell, J.A., Vaughan, D.J., and Johnson, K.H. (1974) The electronic structure of rutile, wüstite, and hematite from molecular orbital calculations. American Mineralogist, 59, 319–334.

Trautwein, A.X., Kreber, E., Gonser, U., and Harris, F.E. (1975) Molecular orbital and Mössbauer study of iron-oxygen compounds. Journal of Physics and Chemistry of Solids, 36, 325–328.

Trautwein, A.X., Bill, E., Bläs, R., Lauer, S., Winkler, H., and Kostikas, A. (1985) Iron sulfur and iron molybdenum sulfur compounds: Comparison of molecular orbital calculations and spin-Hamiltonian analysis of Mössbauer spectra. Journal of Chemical Physics, 82, 3584–3593.

Winkler, H., Eisberg, R., Alp, E., Ruffer, R., Gerdau, E., Lauer, S., Trautwein, A.X., Grodzicki, M., and Vera, A. (1983) Pure nuclear reflexes and combined hyperfine interactions in YIG. Zeitschrift für Physik B, 49, 331–341.